Ecological Modelling 457 (2021) 109678

Contents lists available at ScienceDirect

Ecological Modelling

journal homepage: www.elsevier.com/locate/ecolmodel

Spatial patterns of correlation between conspecific species and size diversity in forest ecosystems

Hongxiang Wang [a], Xiaohong Zhang [b,*], Yanbo Hu [c,*], Arne Pommerening [d]

[a] College of Forestry, Guangxi University, Nanning 530004, China
[b] Key Laboratory of Forest Management and Growth Modelling, NFGA, Chinese Academy of Forestry, Research Institute of Forest Resource Information Techniques (IFRIT), Beijing 100091, China
[c] Key Laboratory of Tree Breeding and Cultivation of National Forestry and Grassland Administration, Research Institute of Forestry, Chinese Academy of Forestry, Box 1958, Beijing 100091, China
[d] Faculty of Forest Sciences, Department of Forest Ecology and Management, Swedish University of Agricultural Sciences SLU, Skogsmarksgränd 17, Umeå SE-901 83, Sweden

ARTICLE INFO

Keywords:
Mingling-size hypothesis
Diversity indices
Correlation space
Neighbourhood indices
Size dominance
Forest development stage
Diversity loss

ABSTRACT

Recently correlations between spatial species and size diversity have been found in many forest ecosystems around the world. They are likely to play a prominent role in nature's mechanisms of maintaining species and size diversity. In this study, we analysed the species population means of spatial species-mingling and size-inequality indices in 36 large forest monitoring plots from the temperate and subtropical zones in China. Based on the literature we included eleven diversity-index combinations and considered their correlations for increasing numbers of nearest neighbours. Generally, positive correlations are related to between-species population size differences whilst negative correlations reflect within-species population size differences. Our results showed that the selected species-mingling and size-inequality indices produced different correlation patterns in one and the same monitoring site. We therefore defined a species-mingling size-inequality correlation space by computing the 0.025 and the 0.975 quantiles from the correlation data of the eleven index combinations. We noticed that each observed correlation space included 1–3 combinations of five basic geometric types and can be interpreted as the unique signature of a forest ecosystem in time. The correlation space allowed us to understand more clearly at which spatial scale within-species correlation was more influential than between-species inequality and vice versa. The shape of the correlation space is interpretable and gives important clues about the forest development stage of a forest ecosystem.

1. Introduction

Studying species diversity for a very long time has been the most prominent direction of biodiversity research (Gaston and Spicer, 2004). Only fairly recently it has been recognised that size diversity or size inequality matters, too, since with some plant species, such as tree species, individuals can markedly differ in size (Ford, 1975; Weiner and Sobrig, 1984). It turned out to be even more insightful to analyse species and size diversity jointly: Pommerening and Uria-Diez (2017) and Wang et al. (2018) independently discovered that in many forest ecosystems larger trees often tend to be surrounded by tree species different from their own and termed this the *mingling-size hypothesis*. This discovery provided incentives to study spatial species-size correlations in greater detail in order to understand more clearly how species and size diversity are maintained naturally.

From earlier studies we reported correlations between spatial species mingling and size inequality (Wang et al., 2020; Pommerening et al., 2020a,2021). These correlations were discovered at forest ecosystem level and do not necessarily have to exist when analysing individual species populations. If they, however, occurred in species populations as well, this would give a vital clue as to how the natural mechanisms of maintaining tree diversity work and how they are broken down into small spatial units of the forest ecosystem. Therefore this study focused on species-size correlations among nearest neighbours in species populations. In pursuing this objective, we applied methods of point process statistics, where the variability of spatial point patterns is studied. In our case, the points were defined as stem-centre coordinates of trees and the species and size information constituted so-called marks (Pommerening

* Corresponding authors.
E-mail addresses: zhangxh@ifrit.ac.cn (X. Zhang), hyanbo@caf.ac.cn (Y. Hu).

https://doi.org/10.1016/j.ecolmodel.2021.109678
Received 22 March 2021; Received in revised form 17 May 2021; Accepted 22 July 2021
Available online 12 August 2021

and Grabarnik, 2019), i.e. additional information associated with the points which may help to explain the point pattern.

In previous studies we learned that there are often correlations between mean spatial species mingling and mean measures of spatial size inequality of the species populations in the same woodland. Our original idea therefore was to study these correlations for only one pair of spatial species and size inequality indices in greater detail, namely Eqs. (1) and (4) in Table 1, and to see what they imply and what they depend on. While engaging in such an analysis, we realised that the problem is in fact more complex, since correlations, as expected, not only varied with the neighbourhood size, but also with different index combinations. In the monitoring plot at Jiaohe (Jilin Province, see Section 2.2), plot d, (Fig. 1A), for example, using $k = 5$ nearest neighbours the correlations of eleven species mingling – size inequality index combinations from Table 1 were all positive and therefore the results were fairly consistent. Only the strength of the relationship differed between indices. This, however, was not the case at Jingouling (also Jilin Province), plot l (Fig. 1B), where only three index combinations were positively and eight were negatively correlated. The results indicated that even the general trends of species-size interactions were not consistent at this site.

From these and similar results we concluded that correlations between diversity indices can only be fully understood, if several of them were considered simultaneously. Such an analysis strategy is also consistent with the textbook recommendation to always apply several seemingly competitive characteristics (Illian et al., 2008; Torquato, 2002; Pommerening and Grabarnik, 2019). Therefore we decided to include all known characteristics relating to spatial species mingling and size inequality. As a result we obtained an area or space that includes all correlations and their dependence on distance r, which – in analogy to the parameter space of models – we termed *correlation space*.

Accordingly the objective of this study was to map – as much as possible – the whole correlation space of spatial species mingling and size inequality by simultaneously varying neighbourhood size and index combinations. Our hypotheses were that (1) this mapping would result in shapes of correlation space characterising the relationship between spatial species mingling and size inequality and (2) that these shapes can then be ecologically interpreted.

2. Materials and methods

2.1. Spatial diversity indices

Based on the literature we identified three indices relating to species mingling (Eqs. (1)–(3)) and six indices relating to size inequality (Eqs. (4)–(9)). The species-specific variants of each index were calculated by limiting subject trees i to the individuals of the species under consideration whilst the k nearest neighbours were the "natural" neighbours of each subject tree according to Euclidean distance and regardless of species. This definition of neighbourhood is crucial to the interpretation of the correlation results.

Gadow (1993) defined *spatial species mingling* as the mean heterospecific fraction of plants among the k nearest neighbours of a subject plant i (Eq. (1) in Table 1). Due to the discrete nature of outcomes for a given k there are only $k + 1$ possible values, M_i can take, i.e. $0/k$, $1/k$, …, k/k, where the number in the numerator denotes the number of neighbours with a species different from that of tree i. All index values lie between 0 and 1.

In analogy to Pielou's segregation index (Pielou, 1977) *species segregation* Ψ has been suggested by Pommerening and Uria-Diez (2017). Here mean population mingling $\overline{M}$ is divided by expected species mingling, $\mathbf{E}M$, (Eq. (2) in Table 1). $\Psi = 0$, if the species marks are spatially uncorrelated. If the nearest neighbours and a given tree always tend to share the same species, Ψ is positive with a maximum at $\Psi = 1$. If all neighbours always tend to have a species different from that of the tree under study, Ψ is negative with a minimum at $\Psi = -1$.

Hui et al. (2008) and (2011) proposed the *richness-weighted mingling index* M_i' (Eq. (3) in Table 1) as an extension of the original mingling index by Gadow (1993) by merging the concept of species mingling with the concept of species richness. Accordingly each M_i (from Eq. (1)) is multiplied by the species richness s_i among the k nearest neighbours. We amended the index definition by introducing term c in Table 1 to ensure that the number of species that are theoretically possible in a group of $k + 1$ trees are considered correctly. Both the species segregation and the richness-weighted mingling index are less dependent on overall population species richness than the original mingling index. Values of M_i' are generally smaller and take a larger range of different values than those of M_i.

Gadow (1993) defined *size differentiation* (Eq. (4) in Table 1) as the mean ratio of smaller-sized and larger-sized marks of the k nearest

Table 1
Definitions of the spatial species-mingling and size-inequality indices used in this study.

Eq.	NNSS	Diversity of	Formula	Variable definitions
(1)	Species mingling (Gadow, 1993)	Species	$M_i = \frac{1}{k}\sum_{j=1}^{k} \mathbf{1}(\text{species}_i \neq \text{species}_j)$	$\mathbf{1}(\text{A}) = 1$, if A is true, otherwise $\mathbf{1}(\text{A}) = 0$
(2)	Species segregation (Pommerening and Uria-Diez, 2017)	Species	$\Psi = 1 - \frac{\overline{M}}{\mathbf{E}M}$	Population mean $\overline{M}$ of Eq. (1) divided by expected mingling and subtracted from 1
(3)	Weighted species mingling (Hui et al., 2011)	Species	$M_i' = \frac{1}{k \cdot c}\sum_{j=1}^{k} \mathbf{1}(\text{species}_i \neq \text{species}_j) \cdot s_i$	s_i – species richness among the k nearest neighbours of and including tree i; $c = \min(S, k + 1)$, where S – total species richness of forest stand
(4)	Size differentiation (Gadow, 1993)	Size	$T_i = 1 - \frac{1}{k}\sum_{j=1}^{k} \frac{\min(m_i, m_j)}{\max(m_i, m_j)}$	m_i – size of subject tree i, m_j – size of neighbour j
(5)	Size segregation (Pommerening and Uria-Diez, 2017)	Size	$\text{Y} = 1 - \frac{\overline{T}}{\mathbf{E}T}$	Population mean $\overline{T}$ of Eq. (4) divided by expected differentiation and subtracted from 1
(6)	Size dominance (Aguirre et al., 2003)	Size	$U_i = \frac{1}{k}\sum_{j=1}^{k} \mathbf{1}(\text{m}_i > \text{m}_j)$	See previous definitions
(7)	Weighted size dominance	Size	$U_i' = \frac{1}{\sum_{j=1}^{k} m_j}\sum_{j=1}^{k} \mathbf{1}(\text{m}_i > \text{m}_j) \cdot m_j$	See previous definitions
(8)	Size dominance differentiation (Albert, 1999)	Size	$U_i'' = \frac{1}{k}\left(\sum_{j=1}^{k} \mathbf{1}(\text{m}_i > \text{m}_j)\left(1 - \frac{m_j}{m_i}\right) - \sum_{j=1}^{k} \mathbf{1}(\text{m}_i < \text{m}_j)\left(1 - \frac{m_i}{m_j}\right)\right)$	See previous definitions
(9)	Hyperbolic tangent index (Pommerening et al., 2020b)	Size	$T_i' = \frac{1}{k}\sum_{j=1}^{k} \frac{m_i}{m_i + m_j}$	For simplicity we chose to use $\alpha = 0.5$ so that all size marks m are raised to the power of 1, see Pommerening et al. (2020b, p. 3)

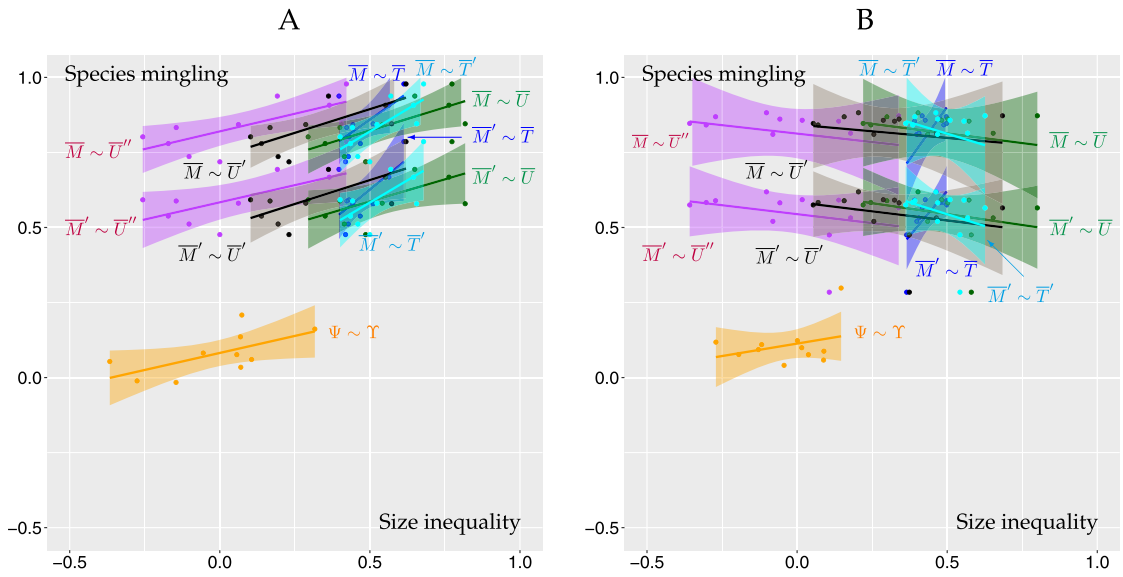

Fig. 1. Exploring the correlations of eleven mean population species and inequality indices (based on stem diameter) using linear regression and 95%-confidence intervals. A: Jiaohe (Jilin Province), plot d. B: Jingouling (Jilin Province), plot l. The diversity indices are defined in Table 1 and $k = 5$ nearest neighbours were used.

neighbours subtracted from one. Size differentiation produces continuous results between 0 and 1 and T_i increases with increasing average size difference between neighbouring trees.

Based on size differentiation (Eq. (4) in Table 1), Pommerening and Uria-Diez (2017) proposed *size segregation* Υ (Eq. (5) in Table 1) in analogy to species segregation Ψ. Υ = 0, if the size marks are independently dispersed without any spatial correlation. If the sizes of nearest neighbours and a given tree are always of similar magnitude, Υ ≈ 1. If all neighbours always tend to have size marks quite different from that of the reference tree, Υ is negative and tends towards –1 in the extreme case.

The *size dominance index* (Eq. (6) in Table 1) was introduced by Hui et al. (1998) and Aguirre et al. (2003) and gives the proportion of k nearest neighbours dominated by tree i. The index draws on similarities with the construction of the mingling index, thus transforming a continuous variable into a binary one and also produces only k +1 possible U_i values.

A new size-inequality index designed in this study is the *weighted size dominance* U_i' (Eq. (7) in Table 1). In contrast to Eq. (6) this index takes advantage of the continuous nature of size variables. Here U_i (from Eq. (6)) is multiplied by mark m_j of the k nearest neighbours and divided by the sum of marks of all neighbours (excluding that of tree i). In other words, U_i' basically is the mark percentile of tree i, i.e. the mark proportion of trees among the k nearest neighbours that are smaller than subject tree i.

Albert (1999) suggested a combination of differentiation and dominance index, the *size dominance differentiation*, U_i'' (Eq. (8) in Table 1). Here the size differentiation of larger neighbours relative to subject tree i is subtracted from the size differentiation of smaller neighbours relative to tree i. As a consequence the continuous value of U_i'' can be between -1 and 1. Negative values of U_i'' indicate that tree i is suppressed by its neighbours. The more positive the values of U_i'' the more dominant is tree i.

Finally Pommerening et al. (2020b) defined the *hyperbolic tangent index* T_i'. The index is based on trigonometric principles and the simplest variant is given in Eq. (9) in Table 1, where the mode parameter α was set to 0.5, so that the exponents of the size marks take the value of 1 and as a result the index calculation simplifies to Eq. (9). Like most indices in Table 1, the index values lie between 0 and 1. The larger the value of T_i' the larger the size dominance of tree i.

These nine species- and size-diversity indices were included in our correlation analyses.

2.2. Study area and data

Daqingshan forest region (abbreviated as D) forms a part of the Daqingshan Forest Farm (22°17′ N, 106°42′ E) of the Experimental Centre of Tropical Forestry, Chinese Academy of Forestry. The research area is situated in Pingxiang city, Guangxi province, which is close to the border between China and Vietnam. The average annual rainfall varies between 1261 and 1695 mm and the average annual temperature is 20.5–21.7 °C. The soil is mainly classified as laterite and red soil. Plot *a* and plot *b* in Daqingshan, abbreviated as Da and Db, are dominated by *Cunninghamia lanceolata* (Lamb.) Hook. mixed with diverse broadleaved species such as *Mytilaria laosensis* Lec., *Macaranga denticulata* (Bl.) Muell. Arg., *Schefflera octophylla* (Lour.) Harms., *Machilus chinensis* (Champ. ex Benth.) Hemsl. and *Castanopsis hystrix* Miq (Wang et al., 2020).

A typical temperate mixed-species forest including coniferous and broad-leaved trees dominates *Jiaohe forest region* (abbreviated as J). The study area is an experimental forest situated in the Dongdapo Nature Reserve (43°51′–44°05′ N, 127°35′–127°51′ E), Jilin province, northeastern China. Average annual rainfall is 700–800 mm and mean annual temperature is 3.5 °C. The soil is dark brown forest soil. Four plots from the *Jiaohe forest region* were included in this study. The first stand, denoted as Ja, is a mixed *Tilia mandschuria-Pinus koraiensis* forest. The second stand, denoted as Jb, can be described as a mixed *Fraxinus mandshurica-Juglans mandshurica* forest. The stand in the third plot, denoted as Jc, is a mixed *Juglans mandshurica-Abies holophylla* forest. The fourth plot, denoted as Jd, represents a mixed forest of *Juglans mandshurica* and *Fraxinus mandshurica* (Pommerening et al., 2019).

Jingouling Experimental Forest Farm (43°17′–43°25′ N, 130°5′–130°20′ E) is situated in Jilin Province, China, and forms a part of the LaoyeLing Mountain in the Changbai Mountain Range. The annual rainfall is 600–700 mm and the mean annual temperature is 4.0 °C. The soil is classified as a dark brown soil with a loamy texture, an acidic pH range and large humus accumulation. This area mainly has secondary spruce-fir-broadleaf mixed forest dominated by Dragon spruce (*Picea asperata* Mast.), Manchurian fir (*Abies nephrolepis* (Trautv. ex Maxim.) Maxim.), Changbai larch (*Larix olgensis* A.Henry) and Korean pine (*Pinus koraiensis* Siebold & Zucc.) among others. The stands included in this research are plots a-l in Jingouling, abbreviated as JGa-JGl.

Jiulongshan Forest (abbreviated as JS) is located in the western suburbs of Beijing (39°57′ N, 116°05′ E) in the northern branch of Taihang

Mountain. Mean annual rainfall is 623 mm and mean annual temperature is 11.8 °C. The site has a thin brown rocky mountain soil with high stone content. In this study, we included forest stands *a* and *b* in Jiulongshan, abbreviated as JSa and JSb. Stand JSa is dominated by planted *Platycladus orientalis* (L.) Franco and is mixed with some naturally regenerated species such as *Quercus variabilis* Blume, *Broussonetia papyrifera* (L.) Vent., *Ailanthus altissima* (Mill.) Swingle, *Prunus davidiana* Carr. and *Gleditsia sinensis* Lam. Stand JSb represents a secondary, mixed-species broadleaved deciduous forest, where the main species *Pinus tabuliformis* Carr. and *Larix principis-rupprechtii* Mayr were planted (Pommerening et al., 2019).

Leye forest region (abbreviated as Ly) is part of the Yachang Nature Reserve situated in Baise City, Guangxi Zhuang Autonomous Region (24°37′–25°00′ N, 106°08′–106°23′ E). The annual rainfall is 1058 mm and the annual average temperature is 16.8 °C. The soil is classified as yellow mountain soil. Dominant species in this forest include Taiwanese sweetgum (*Liquidambar formosana* Hance), Rhododendron (*Rhododendron cavalerie* H. Lév) and Eurya (*Eurya impressinervis* Kobuski, J. Arnold Arbor.). The forest included a large number of small trees growing in close proximity.

Tazigou Experimental Forest Farm (43°05′–43°40′ N, 129°56′–131°04′ E) is located in Jilin Province, China (Pommerening et al., 2021). This area of secondary forest, abbreviated as TF, is situated on Laoyeling Mountain of the Changbai Mountain range. Annual rainfall is between 600 mm and 700 mm and the average annual temperature is 3.9 °C. The area has predominantly dark brown soil (humic cambisols) with a high natural fertility. The main tree species are Mongolian oak (*Quercus mongolica* Fisch. ex Ledeb.), Asian white birch (*Betula platyphylla* Sukaczev), Korean pine (*Pinus koraiensis* Siebold & Zucc.), Ussuri popular (*Populus ussuriensis* Komarov) and Amur lime (*Tilia amurensis* Rupr.). The stands included in this research are plots a-l in Tazigou, abbreviated as TFa-TFl.

Xiaolongshan Forest (abbreviated as XS) is located in the Xiaolongshan Nature Reserve, Gansu province, north-west China. The forest is situated in the north-facing slopes of the West Qinling Mountain range (33°30′–34°49′ N, 104°22′–106°43′ E) and constitutes a natural mixed pine-oak forest. The mean annual rainfall of the study area is 600–900 mm and mean annual temperature is between 7 and 12 °C. The soil type is a grey cinnamon soil in the north of the Qinling Mountains and yellow cinnamon soil prevails in the south. Four plots from the Xiaolongshan Forest were included in this study. The first stand denoted as XSa is a mixed pine-oak forest and is mainly composed of *Quercus aliena* var. *acuteserrata* Maxim., *Pinus armandii* Franch. and *Dipteronia sinensis*. The second stand, XSb, is also a mixed pine-oak population dominated by *Quercus aliena* var. *acuteserrata* Maxim., *Ulmus glabra* Huds. and *Symplocos paniculata* (Thunb.) Wall. ex D. Don. The third stand, XSc, is a natural deciduous broad-leaved mixed forest and *Quercus aliena* var. *acuteserrata* Maxim., *Dendrobenthamia japonica* (DC.) fang. var. *chinensis* and *Acer davidii* Franch. are the most abundant species. The fourth stand (XSd) is mainly dominated by *Quercus aliena var. acuteserrata* Maxim., *Pinus armandii* Franch. and *Acer davidii* Franch (Pommerening et al., 2019). The plot locations are shown in Fig. 2.

2.3. Analysis

For each forest plot we calculated the population means of all diversity indices in Table 1 separately for all species populations that have more than 20 individuals, which appeared to be a reasonable lower threshold. Stem diameter at breast height (measured at 1.3 m above soil level) was used as size characteristic throughout this study, however, any size variable or combinations of size variables can be included in similar work. In calculating the species-population means we varied the number of nearest neighbours k from 1 to 50 and applied the NN1 edge correction (Pommerening and Stoyan, 2006). Even $k = 50$ did not exceed an intertree-distance range of 15 m in the dense woodlands we studied, see Section 2.2. For each number of k we calculated Pearson's correlation index for combinations of mingling and size indices and recorded the mean distance between tree i and the kth nearest neighbour. The index combinations we considered were $\overline{M} \sim \overline{T}$ (Eqs. (1), (4)), $\overline{M}' \sim \overline{T}$ (Eqs. (3), (4)), $\Psi \sim Y$ (Eqs. (2), (5)), $\overline{M} \sim \overline{U}$ (Eqs. (1), (6)), $\overline{M}' \sim \overline{U}$ (Eqs. (3), (6)), $\overline{M} \sim \overline{U}'$ (Eqs. (1), (7)), $\overline{M}' \sim \overline{U}'$ (Eqs. (3), (7)), $\overline{M} \sim \overline{U}''$ (Eqs. (1), (8)), $\overline{M}' \sim \overline{U}''$ (Eqs. (3), (8)), $\overline{M} \sim \overline{T}'$ (Eqs. (1), (9)) and $\overline{M}' \sim \overline{T}'$ (Eqs. (3), (9)). For each of these eleven pairs we had distance-dependent correlation values corresponding to 50 different values of k. We used a non-parametric Gaussian kernel estimator with bandwidth $h = 2$ to construct non-parametric trend curves for each of the eleven index relationships to comprehensively map the total correlation space between spatial species mingling and size inequality. To determine the outer contour lines of the correlation space, all spatially explicit correlation results of the eleven relationships were merged and from this merged data set we computed the 0.025 and 0.975 quantiles. We again applied a non-parametric Gaussian kernel estimator (this time with bandwidth $h = 3$) to the quantile data to define the shape of the correlation space. When examining the graphical results of the correlation space between spatial species mingling and size inequality for each monitoring plot, we realised that the 0.025 and 0.975 quantiles defined recurrent shapes that could be used for classification and

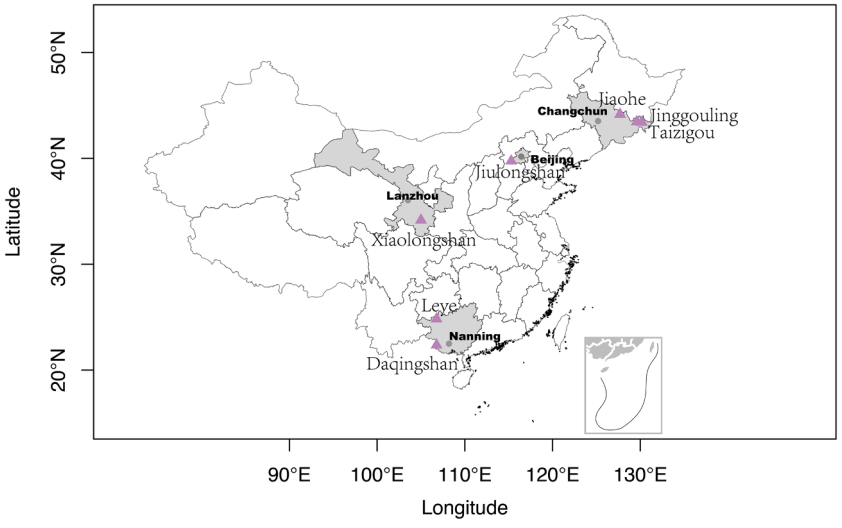

Fig. 2. Map of forest monitoring plot locations in China.

interpretation.

The shapes shown in Fig. 3 represent the basic correlation patterns observed in the forest monitoring plots we studied. These idealised shapes are generic and likely to apply to many other woodlands across the temperate and subtropical climate zones. Often the observed patterns tend to be a combination of two or more shapes and/or the boundaries deviate from linearity.

Classifying the observed patterns according to the five types of Fig. 3 facilitates the interpretation of ecological processes in the respective forest ecosystems. In general, strong *positive correlations* between spatial species mingling and size inequality implies that specimens of different species mingle at that scale that also have very different sizes whilst the sizes *within* specimens of the same species do not differ much (Pommerening et al., 2021). Strong *negative correlations* on the other hand suggest that the sizes *between* specimens of different species are rather similar but that size diversity is high *within* specimens of the same species at that spatial scale. Positive and negative correlations of the same absolute magnitude therefore describe very different *qualities of spatial interaction*. For the relationship $\Psi \sim Y$ in parts slightly different interpretations apply due to the specific definitions of the indices involved.

Increasing distance implies that tree neighbourhoods become larger. Since distance and neighbourhood size in Fig. 3 increase vertically from the bottom up, the shapes shown in Figs. 4 and 5 also need to be interpreted that way. We found that the requirement to interpret the correlation-space shapes in the direction of increasing distance markedly reduced interpretation and classification ambiguity. According to this requirement we labelled mixed or transitional shapes in such a way that the first letter represents the prevailing type at short distances and the following letter(s) indicate the pattern at larger distances.

Correlation shape A describes situations where correlations are initially both high and low (or negative) at short distances and with increasing distance (= neighbourhood size) tend to converge towards the symmetry axis (median) of the correlation space which often is at $r' = 0$, but can also occur at any other positive or negative correlation value. In most cases this implies that correlations are strongest or weakest when only the immediate neighbourhood involving short distances is considered.

Shape B reverses shape A. Here the correlation coefficients approach the median or symmetry axis of the correlation space at short distances and as distances increase the shape then opens like a funnel implying that correlations both increase and decrease (or become negative) with distance. This usually means that correlations between spatial species and size mingling are both stronger and weaker (or negative) when larger neighbourhoods are considered. Shapes A and B describe situations where the spatial correlation patterns at a particular distance *r* are not consistent across the range of spatial indices listed in Table 1. In the case of shapes A and B, the median/the symmetry axis of the correlation space is approximately constant throughout the distance range.

Shape C implies a gradual shift in correlation with increasing neighbourhood size and distance, e.g. from high to low or from positive to negative correlation values. This can mean that correlations between spatial species and size mingling are strong when only the immediate neighbourhood at short distances is considered and then weaken when more neighbours are involved. The shape can also imply that the quality of relationship is reversed, i.e. that predominantly positive correlations turn into negative ones.

Shape D is the opposite of shape C implying a gradual shift from low to high or from negative to positive correlations with increasing neighbourhood size and distance. Shapes C and D describe situations with spatial correlations that are more or less consistent across the range of spatial indices listed in Table 1 but differ with *r*. The gradual shift also affects the median/the symmetry axis of the correlation space in shapes C and D, i.e. the median varies with increasing neighbourhood size.

Finally shape E describes situations where the correlation space is more or less constant with increasing or decreasing neighbourhood size. The median correlation coefficient/the symmetry axis of the correlation space can be near 0, but can also be located elsewhere whilst being approximately constant/parallel to the ordinate throughout the distance range. This pattern suggests species and size correlations that are largely independent of spatial scales. Across all spatial indices in Table 1 and across all spatial scales the correlations between species mingling and size inequality are largely consistent.

All calculations were carried out using our own R scripts (version 3.6.3; R Development Core Team, 2020) and the `spatstat` (Baddeley et al., 2016) package.

3. Results

3.1. Basic statistics

All research plots are located at upland sites and elevation varies from 600 m (Jd) to 1880 m asl (XSd). Densities in the 36 plots ranged from 746 in Jb to 5804 trees per hectare in plot Ly. The minimum number of species observed was 9 in plots TFb and TFd, whilst the maximum was 86 in Ly. Mean arithmetic diameter at breast height (*dbh*) was smallest at Ly (5.8 cm) and largest at Jc (18.3 cm). The coefficient of variation had a minimum at JSb with 0.39 and a maximum at Ly with 1.42.

Basal area ranged from 13.9 m^2 (TFf) to 45.9 m^2 (Ly) per hectare. Mean species mingling for both indices was lowest at JSb ($\widehat{M} = 0.43$, $\widehat{M}' = 0.19$) and highest at Jc ($\widehat{M} = 0.83$, $\widehat{M}' = 0.59$). It is also at JSb where mean size differentiation is lowest ($\widehat{T} = 0.33$) and at TFj and TFl size differentiation is highest ($\widehat{T} = 0.53$). These values indicate generally high species mingling, whilst size inequality is moderate.

3.2. Correlation space

Already at first glance it is evident that there is a high diversity of correlation curve shapes. In some cases such as Jb, JGg, JGi, JGk, Ly (Fig. 4) and TFh, TFj, TFh, TFj, XSa, XSb (Fig. 5) the correlation space is more or less fully filled with index correlation curves. With other monitoring plots, notably in the case of Da and Db, there are larger gaps in the correlation space. For some plots the index correlation curves largely run in parallel one to another, for others they intersect.

While the former behaviour suggests that correlation does not depend much on distance and neighbourhood size, in the latter case correlation changes with distance. Correlations can both increase and

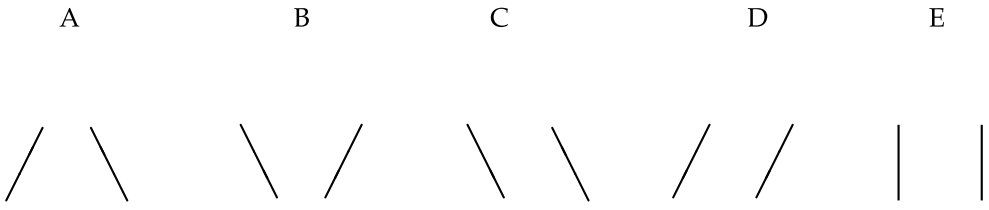

Fig. 3. Idealised shape types formed by the 0.025 and 0.975 quantiles of the correlation data and describing the spatial species mingling – size inequality correlation space. For visual clarity axes were omitted and for each shape distance increases in vertical direction and correlations become more positive in horizontal direction.

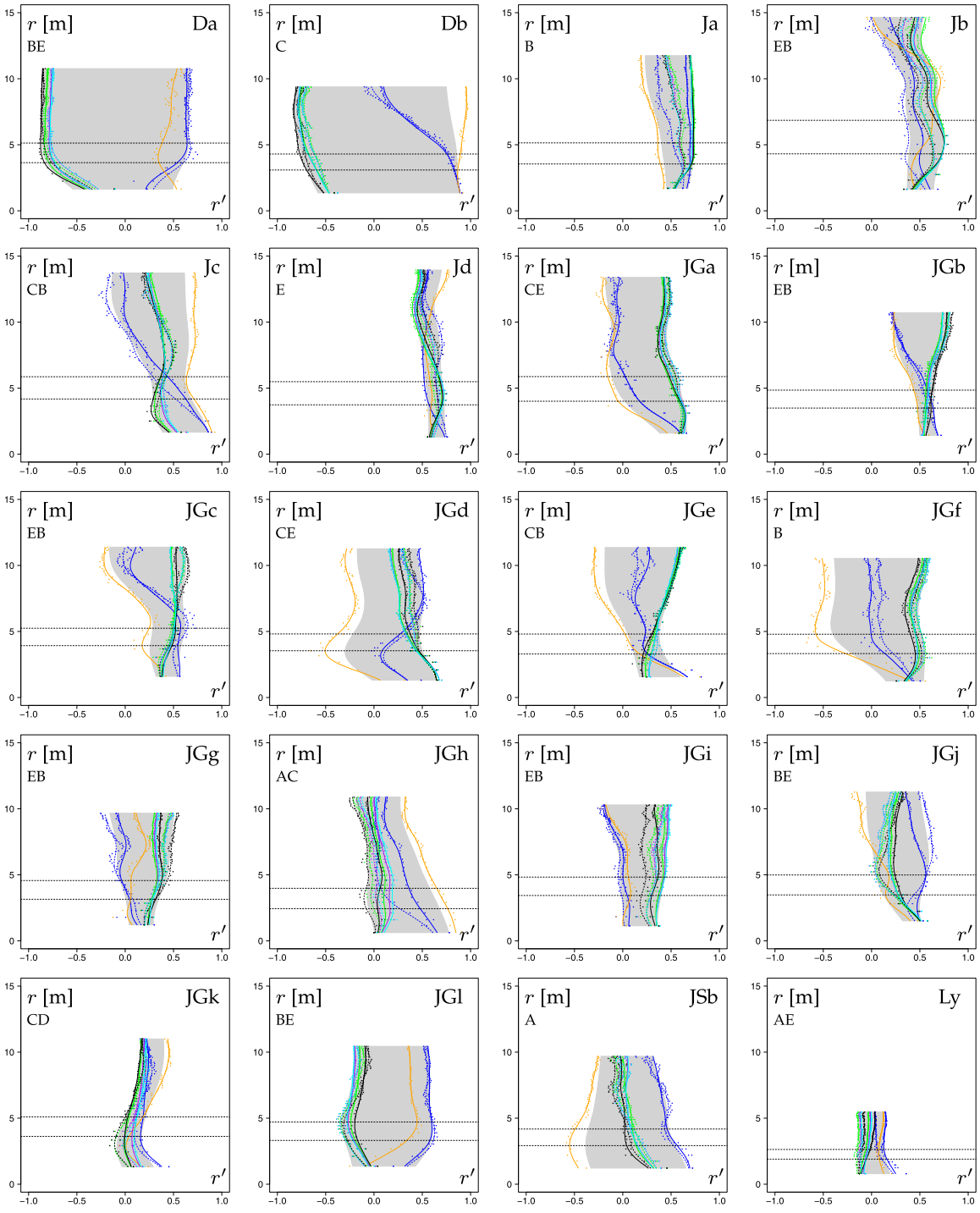

Fig. 4. Correlations r' between spatial species mingling and spatial size inequality depending on distance r in research plots Da, Db, Ja – Jd, JGa – JSb and Ly. The trend curves were estimated using non-parametric Gaussian kernel estimator (bandwidth $h = 2$). Index combinations from Table 1 considered: $\widehat{M} \sim \widehat{\overline{T}}$ (blue continuous), $\widehat{M}' \sim \widehat{\overline{T}}$ (blue dashed), $\widehat{\Psi} \sim \widehat{Y}$ (orange), $\widehat{M} \sim \widehat{\overline{U}}$ (green continuous), $\widehat{M}' \sim \widehat{\overline{U}}$ (green dashed), $\widehat{M} \sim \widehat{\overline{U}}'$ (black continuous), $\widehat{M}' \sim \widehat{\overline{U}}'$ (black dashed), $\widehat{M} \sim \widehat{\overline{U}}''$ (purple continuous), $\widehat{M}' \sim \widehat{\overline{U}}''$ (purple dashed), $\widehat{M} \sim \widehat{\overline{T}}'$ (cyan continuous) and $\widehat{M}' \sim \widehat{\overline{T}}'$ (cyan dashed). The light-grey areas highlight the correlation space between the 0.025 and 0.975 quantiles of the eleven relationships estimated with a non-parametric Gaussian kernel estimator (bandwidth $h = 3$). The two dashed horizontal lines denote the mean distance between a subject tree and its $k = 5$th and $k = 10$th nearest neighbour.

decrease with distance. Marked changes in correlation with distance are often responsible for the formation of mixed types of correlation space that include more than one letter from Fig. 3. In plot Db (Fig. 4), for example, correlations $\widehat{M} \sim \widehat{\overline{T}}$ and $\widehat{M}' \sim \widehat{\overline{T}}$ are very high for small distances and then dramatically decrease towards zero while r approaches 10 m. For the same index correlations an opposite trend can be observed in plot Da (Fig. 4). Here correlations are very low for short distances or low numbers of indices and then increase towards 0.5 at $r = 5$ m. A further increase of distance does not change the correlation strength. In rare occasions, initially positive correlations cross over to become negative correlations. This is often associated with pattern C (Fig. 3),

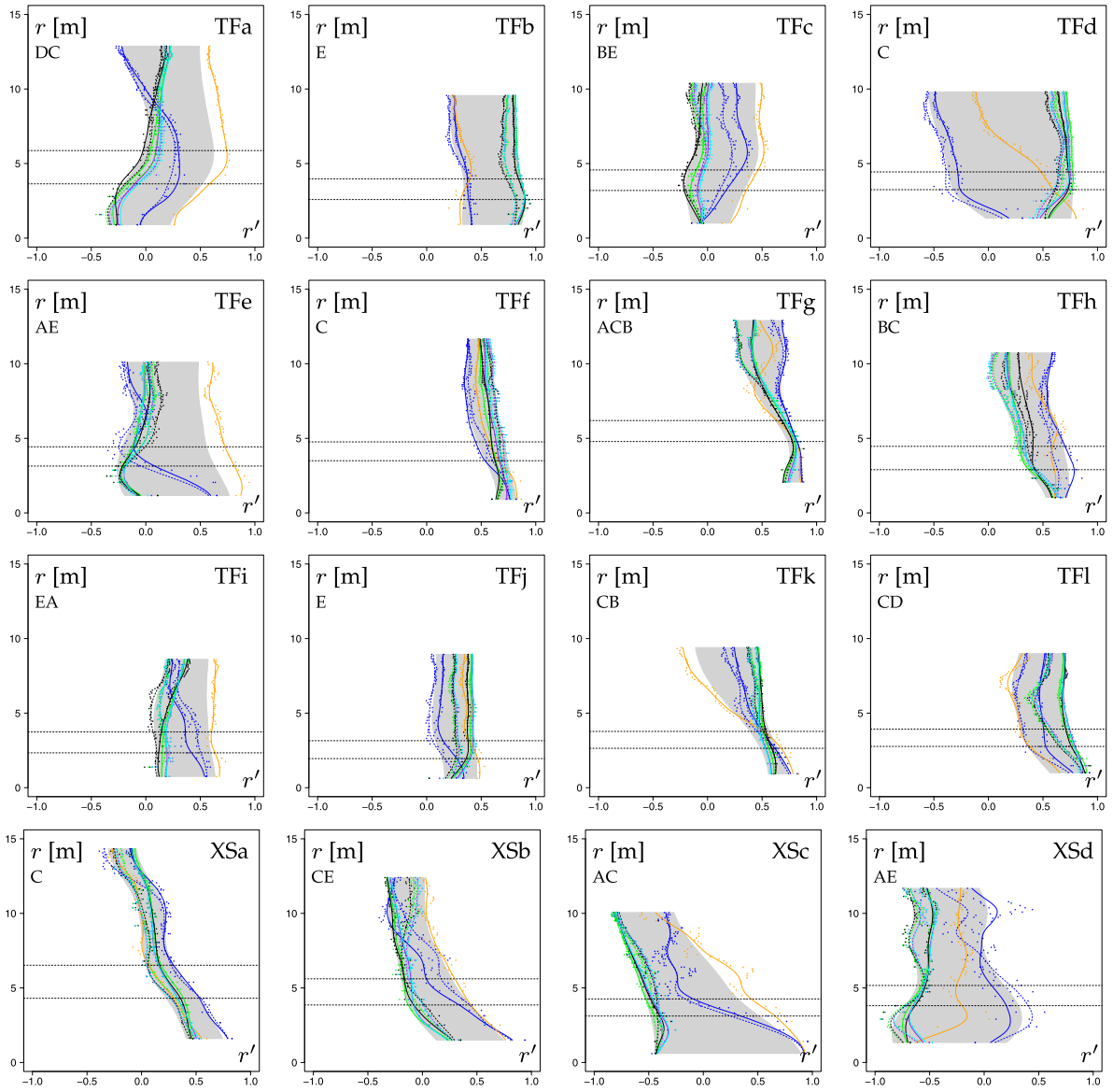

Fig. 5. Correlations r' between spatial species mingling and spatial size inequality depending on distance r in research plots TFa – TFl and XSa – XSd. The trend curves were estimated using non-parametric Gaussian kernel estimator (bandwidth $h = 2$). Index combinations from Table 1 considered: $\widehat{M} \sim \widehat{T}$ (blue continuous), $\widehat{M}' \sim \widehat{T}$ (blue dashed), $\widehat{\Psi} \sim \widehat{Y}$ (orange), $\widehat{M} \sim \widehat{U}$ (green continuous), $\widehat{M}' \sim \widehat{U}$ (green dashed), $\widehat{M} \sim \widehat{U}'$ (black continuous), $\widehat{M}' \sim \widehat{U}'$ (black dashed), $\widehat{M} \sim \widehat{U}''$ (purple continuous), $\widehat{M}' \sim \widehat{U}''$ (purple dashed), $\widehat{M} \sim \widehat{T}'$ (cyan continuous) and $\widehat{M}' \sim \widehat{T}'$ (cyan dashed). The light-grey areas highlight the correlation space between the 0.025 and 0.975 quantiles of the eleven relationships estimated with a non-parametric Gaussian kernel estimator (bandwidth $h = 3$). The two dashed horizontal lines denote the mean distance between a subject tree and its $k = 5$th and $k = 10$th nearest neighbour.

see, for example, correlations $\widehat{M} \sim \widehat{T}$ and $\widehat{M}' \sim \widehat{T}$ in TFa, TFd, XSa (Fig. 5). It is also interesting to note that there is a tendency for correlation-space shapes involving type C to include some strong correlations at short distances, see, for example, Jc, JGh, TFf, TFk, TFl, XSa, XSb and XSc (Figs. 4 and 5). The relationships $\widehat{M} \sim \widehat{T}$ and $\widehat{M}' \sim \widehat{T}$ are very often involved with strong correlations in these monitoring plots.

As mentioned in the Introduction, it is not uncommon that for one and the same monitoring plot some of the index correlations are positive and some are negative, e.g. Da, Db, JGd, JGe, JGf, JGl, JSb, Ly (Fig. 4) and TFa, TFc, TFd, TFe, TFk, XSc, XSd (Fig. 5). There is no trend for any of the index pairings to be always at a particular location in the correlation space, e.g. at the lower or upper boundary. However, the two combinations with the same size-inequality index but different species-mingling measures are usually quite close together, hence we have always assigned the same colour to them.

The pairings $\widehat{M} \sim \widehat{U}$, $\widehat{M}' \sim \widehat{U}$, $\widehat{M} \sim \widehat{U}'$, $\widehat{M}' \sim \widehat{U}'$, $\widehat{M} \sim \widehat{U}''$, $\widehat{M}' \sim \widehat{U}''$, $\widehat{M} \sim \widehat{T}'$ and $\widehat{M}' \sim \widehat{T}'$ often occur close together. This seems to suggest that the index construction is similar or highlights similar aspects of size inequality, whilst combinations involving $\widehat{T}$ and $\widehat{Y}$ often show a different behaviour. In fact the former pairings apparently involve *dominance* indices whilst $\widehat{T}$ and $\widehat{Y}$ include *differentiation* indices. Dominance indices attempt to express how the size of the subject tree relates to that of its neighbours, whilst diversity indices focus on size diversity in the neighbourhood as a whole.

It is also worth noting that the selection of small k, such as $k = 5$ or $k = 10$, is – as suspected – not always a choice that is located near the maximum correlation of a given index combination. At this spatial

location/neighbourhood size correlations can be strong in the case of the BE correlation-space pattern, see, for example, JGl, Da (Fig. 4), TFc (Fig. 5). Fixed $k = 4$ is a popular choice in the literature (Aguirre et al., 2003; Hui et al., 2011) and often seems to miss out on stronger correlations at $k \neq 4$.

The most striking observation is that the shape of the correlation space differs from monitoring plot to monitoring plot, whereby typical patterns are clearly recognizable (Fig. 3) so that each plot can be assigned to one of these typical patterns or to a combination of mostly two types, which supports our first hypothesis. The generic types can be interpreted as explained in Section 2.3.

Overall combinations of correlation types prevail over the basic types defined in Fig. 3. This implies that in the majority of cases correlations are subject to change with distance. Only A, B, C and E occur as basic types. The proportions are quite evenly spread over the range of combinations (see Fig. 6). With 5 monitoring plots out of 36, combination EB is the most common type followed by BE and C. Combination EB implies that correlations are fairly constant with increasing neighbourhood size at first and then increase or decrease at larger distances (see Section 2.3). Rare correlation-space types are A, ACB, BC, DC and EA. However, the differences in absolute frequencies are comparatively small.

4. Discussion

Correlations between spatial species and size diversity are an important notion of forest ecosystems and have until recently not received much recognition. They frequently occur in managed and unmanaged woodlands and form an important part of the mechanisms of natural maintenance of biodiversity in forest ecosystems. These are important to understand in order to actively mitigate the adverse effect of climate change on biodiversity through appropriate forest management. In pursuit of a better understanding of these natural mechanisms, we analysed correlations between species population means of spatial species and size diversity that coexist in the same woodland. 36 large monitoring plots from China with a minimum of 9 and a maximum of 86 species (see Table 2) were examined for these correlations. In earlier research, we learned that the interaction between conspecific and heterospecific size structure plays a crucial role in these correlations (Wang et al., 2020; Pommerening et al., 2020a,2021): Positive correlations between spatial species mingling and size inequality imply that specimens of different species mingle at that spatial scale that also have very different sizes whilst the sizes within specimens of the same species do not differ much. Negative correlations on the other hand suggest that the sizes between specimens of different species are rather similar but that size diversity is high within specimens of the same species at that spatial scale.

We found that different species mingling and size inequality indices show different correlation patterns in the same woodland. This is plausibly related to the index algorithm and the corresponding focus these diversity indices have, e.g. size diversity as opposed to size dominance of the subject tree. In future studies, more attention should be paid to the distinction between these two inequality measures. For understanding species mingling and size inequality correlations better we included nine different indices resulting in eleven index combinations. By computing the 0.025 and 0.975 quantiles from the combined correlation data we were able to define the species-size inequality correlation space for each of the 36 monitoring plots. When considering the shapes of these correlation spaces, we realised that all of them can be described by relying on five generic types (Fig. 3, hypothesis 1) either as single types or as a combination of 2–3. Each specific shape of the correlation space of a monitoring plot can be understood as the unique signature of a forest ecosystem in time.

In our study, there was a high diversity of different correlation space types and accordingly the proportions of plots were quite evenly spread over the range of combinations. The most common type was EB implying that correlations are initially fairly constant but then increase or decrease at larger distances. Interestingly type C usually involved high correlations of $\widehat{\widehat{M}} \sim \widehat{\widehat{T}}$ and $\widehat{\widehat{M}}' \sim \widehat{\widehat{T}}$ at short distances. With the same type and relationships there were cases where initially positive correlations would cross the symmetry axis of the correlation space to eventually become negative correlations. These are particularly interesting, since for the same monitoring plots the quality of correlation radically changes at different spatial scales, i.e. from between species correlations to within species correlations or vice versa. These relationships highlight that the natural mechanisms of maintaining tree diversity are complex and can result in different patterns at different scales. Size differentiation $\widehat{\widehat{T}}$ is related to the test function of the mark variogram (Pommerening and Grabarnik, 2019) and Motz et al. (2010) found a significant correlation between size differentiation and forest inventory design.

The popular choice of $k = 4$ nearest neighbours is likely to take advantage of absolute correlation maxima only, if the correlation-space

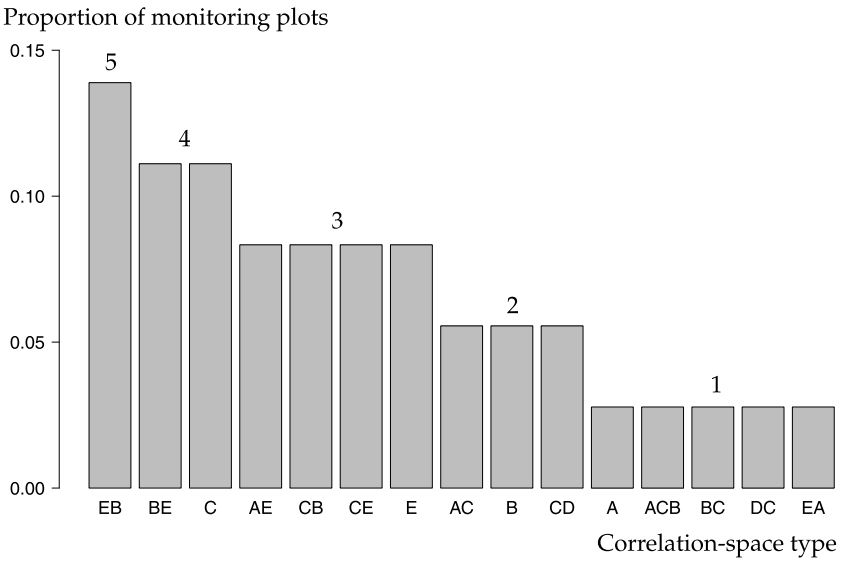

Fig. 6. Proportion of monitoring plots in different correlation-space types (see Fig. 3) in descending order. The numbers over the bars give the absolute numbers of monitoring plots for each type.

Table 2

Basic characteristics of the 36 monitoring plots in China. $\widehat{\overline{M}}$ is the estimated mean mingling index according to Eq. (1), $\widehat{\overline{M}}'$ is the estimated mean weighted mingling index (Eq. (3)), and $\widehat{\overline{T}}$ is the size differentiation index (Eq. (4)) using stem diameter at breast height (*dbh*) as size characteristic. All three indices were calculated for $k = 5$ nearest neighbours using the NN1 edge correction (Pommerening and Stoyan, 2006) and the equations are given in Table 1.

Plot	Slope (°)	Mean altitude (m)	Plot size (m × m)	Density (trees ha^{-1})	Number of species	Mean *dbh* (cm)	*dbh* coeff. of variation	Basal area ($m^2 ha^{-1}$)	$\widehat{\overline{M}}$	$\widehat{\overline{M}}'$	$\widehat{\overline{T}}$
Da	23	725	90 × 110	1445	57	15.4	0.486	33.16	0.78	0.51	0.42
Db	32	710	100 × 80	1766	53	14.8	0.535	39.10	0.73	0.46	0.42
Ja	17	660	100 × 100	1178	20	14.7	0.726	30.42	0.78	0.52	0.43
Jb	9	620	100 × 100	748	21	17.7	0.724	27.95	0.79	0.53	0.45
Jc	9	620	100 × 100	797	19	18.3	0.710	31.67	0.83	0.59	0.46
Jd	9	600	100 × 100	808	19	16.6	0.771	27.80	0.82	0.58	0.46
JGa	3	742	100 × 100	934	12	14.4	0.652	21.69	0.72	0.47	0.46
JGb	5	752	100 × 100	1224	11	12.6	0.757	23.88	0.75	0.47	0.49
JGc	15	760	100 × 100	1233	13	13.2	0.714	25.42	0.78	0.50	0.49
JGd	16	773	100 × 100	1167	13	13.7	0.608	23.68	0.76	0.50	0.45
JGe	5	780	100 × 100	1328	12	13.3	0.608	25.37	0.79	0.52	0.45
JGf	15	792	100 × 100	1422	14	12.7	0.703	27.06	0.74	0.48	0.48
JGg	5	771	100 × 100	1540	13	12.4	0.744	28.90	0.71	0.45	0.49
JGh	5	732	100 × 100	1310	14	12.3	0.774	25.01	0.68	0.40	0.45
JGi	5	749	100 × 100	1438	13	12.3	0.809	28.03	0.68	0.41	0.50
JGj	5	759	100 × 100	1195	13	14.3	0.612	26.37	0.80	0.54	0.46
JGk	5	769	100 × 100	1301	13	13.7	0.627	26.71	0.77	0.52	0.46
JGl	3	773	100 × 100	1437	13	14.0	0.523	28.17	0.72	0.48	0.41
JSb	15	990	100 × 50	1346	12	14.4	0.392	25.44	0.43	0.19	0.33
Ly	19	1700	202 × 86	5804	86	5.8	1.420	45.90	0.72	0.48	0.49
TFa	8	705	100 × 100	1040	12	12.3	0.764	19.51	0.61	0.31	0.45
TFb	8	738	100 × 100	1331	9	10.8	0.782	19.59	0.57	0.28	0.47
TFc	8	675	100 × 100	1344	13	11.3	0.704	20.28	0.60	0.31	0.44
TFd	7	721	100 × 100	1393	9	11.2	0.761	21.68	0.61	0.32	0.46
TFe	10	794	100 × 100	1430	10	12.2	0.790	27.32	0.63	0.33	0.51
TFf	7	645	100 × 100	951	12	10.7	0.793	13.88	0.57	0.29	0.46
TFg	8	637	100 × 100	1226	11	12.0	0.638	19.37	0.58	0.28	0.43
TFh	8	635	100 × 100	1563	10	10.4	0.785	21.60	0.60	0.29	0.46
TFi	7	677	100 × 100	1744	12	8.3	1.022	19.49	0.49	0.23	0.52
TFj	7	685	100 × 100	2209	12	7.9	1.066	23.29	0.61	0.32	0.53
TFk	6	703	100 × 100	1634	11	10.2	0.889	23.86	0.73	0.44	0.52
TFl	10	755	100 × 100	2002	11	7.4	1.213	21.05	0.58	0.28	0.53
XSa	13	1720	70 × 70	841	32	14.8	0.711	21.77	0.82	0.58	0.45
XSb	13	1720	70 × 70	843	35	16.5	0.639	25.35	0.79	0.57	0.46
XSc	17	1650	61 × 50	1584	30	13.9	0.525	30.46	0.71	0.45	0.39
XSd	37	1880	60 × 60	1356	49	12.6	0.594	22.79	0.81	0.57	0.39

type is BE. For other types the absolute maximum is often situated at different k and r. Naturally it is not a requirement to select k in such a way that the correlations between spatial species mingling and size inequality are maximised. However, since the locations of absolute correlation maxima indicate neighbourhood scales where it is very likely that important processes occur, it could be helpful to choose k accordingly.

In this study, the species-mingling size-inequality correlation space has emerged as a new method to identify important neighbourhood processes along with the spatial scales involved. The allocation of the basic types of Fig. 3 is fairly straightforward, although there can be ambiguous cases. However, the introduction of the requirement to interpret the correlation-space shapes in the direction of increasing distance has greatly helped to keep ambiguity to a minimum. In general, the determination of correlation space type much supports the ecological interpretation (hypothesis 2). The shapes of the correlation space can, for example, be related to specific development stages such as those defined by, for example, Oliver and Larson (1996, p. 148f.) and Emborg et al. (2000). Very young forest development stages (stand initiation or formation phase), for example, can be identified from their comparatively short correlation space which often reveals a simple shape involving type E, see, for example, TFi and TFj (Fig. 5). Often correlations here are weak and do not change much with increasing distance and neighbourhood size. Later forest development stages typically have a correlation space extending into the region of larger distances and often exhibit a more complex shape, see, for example, Jb, Jc and XSa (Figs. 4 and 5).

5. Conclusions

The correlations between spatial species mingling and size inequality highlight that the processes causing them are scale dependent and that for different aspects of size inequality, e.g. size diversity versus size dominance, correlations can be very different. The original species mingling and size differentiation indices (Gadow, 1993; Eqs. (1) and (4)) were often involved in the highest correlations. The correlation space newly defined in this study is a promising starting point for a better understanding of natural mechanisms of maintaining tree diversity in forest ecosystems. The concept allows us to see more clearly at which spatial scale within-species size inequality is more important than between-species size inequality. The shape of the correlation space provides pointers as to what forest development stage a forest ecosystem is in and, as a consequence, what processes therefore are currently likely to be the most influential ones. Future studies are necessary to determine how the correlation space changes in time.

Funding

H.W. received funding from the Science and Technology Base and Talent Project of Guangxi (No. AD20297051), and by Guangxi Innovation Driven Development Project (No. AA17204087-8). X.Z. was supported by the National Key R&D Programme of China (2017YFC0504101).

Data accessibility statement

The analysis R source code and the data used in this study are available at https://zenodo.org/record/5167128 or using DOI 10.5281/zenodo.5167128.

CRediT authorship contribution statement

Hongxiang Wang: Conceptualization, Data curation, Formal analysis, Funding acquisition, Writing – original draft, Writing – review & editing. **Xiaohong Zhang:** Data curation, Funding acquisition, Writing – original draft, Writing – review & editing. **Yanbo Hu:** Data curation, Writing – original draft, Writing – review & editing. **Arne Pommerening:** Conceptualization, Formal analysis, Investigation, Methodology, Software, Writing – original draft, Writing – review & editing.

Declaration of Competing Interest

The authors declare that they have no known financial interests or personal relationships that could have influenced the work reported in this paper.

Acknowledgments

Christoph Kleinn granted AP office space and access to printers at his Chair of Forest Inventory and Remote Sensing (Göttingen University, Germany) during the challenging COVID pandemic and Hendrik Heydecke from the same institution supported us by kindly by printing drafts of the manuscript.

References

Aguirre, O., Hui, G.Y., Gadow, K., Jiménez, J., 2003. An analysis of spatial forest structure using neighbourhood-based variables. For. Ecol. Manag. 183, 137–145.
Albert, M., 1999. Analyse der eingriffsbedingten Strukturveränderung und Durchforstungsmodellierung in Mischbeständen. Analysis of Thinning-Induced Changes in stand Structure and Modelling of Thinnings in Mixed-Species Stands. Göttingen University, Hainholz Verlag Göttingen. PhD thesis.
Baddeley, A., Rubak, E., Turner, R., 2016. Spatial point Patterns: Methodology and Applications with R. CRC Press, Boca Raton.
Emborg, J., Christensen, M., Heilmann-Clausen, J., 2000. The structural dynamics of Suserup Skov, a near-natural temperate deciduous forest in Denmark. For. Ecol. Manag. 126, 173–189.
Ford, E.D., 1975. Competition and stand structure in some even-aged plant monocultures. J. Ecol. 63, 311–333.
Gadow, K.v., 1993. Zur Bestandesbeschreibung in der Forsteinrichtung. New variables for describing stands of trees. Forst und Holz 48, 602–606.
Gaston, K.J., Spicer, J.I., 2004. Biodiversity an Introduction. Blackwell Publishing, Oxford.
Hui, G.Y., Albert, M., Gadow, K.v., 1998. Das Umgebungsmaß als Parameter zur Nachbildung von Bestandesstrukturen. Diameter dominance as a parameter for simulating forest structure. Forstwiss. Centralblatt 117, 258–266.
Hui, G., Hu, Y., Zhao, Z., 2008. Evaluating tree species segregation based on neighbourhood spatial relationships. J. Beijing For. Univ. 30, 131–134.
Hui, G., Zhao, X., Zhao, Z., Gadow, K.v., 2011. Evaluating tree species spatial diversity based on neighborhood relationships. For. Sci. 57, 292–300.
Illian, J., Penttinen, A., Stoyan, H., Stoyan, D., 2008. Statistical Analysis and Modelling of Spatial point Patterns. John Wiley & Sons, Chichester.
Oliver, C.D., Larson, B.C., 1996. Forest Stand Dynamics. John Wiley & Sons, New York. Update edition.
Motz, K., Sterba, H., Pommerening, A., 2010. Sampling measures of tree diversity. For. Ecol. Manag. 260, 1985–1996.
Pielou, E.C., 1977. Mathematical Ecology. John Wiley & Sons, New York.
Pommerening, A., Stoyan, D., 2006. Edge-correction needs in estimating indices of spatial forest structure. Can. J. For. Res. 36, 1723–1739.
Pommerening, A., Uria-Diez, J., 2017. Do large forest trees tend towards high species mingling? Ecol. Inform. 42, 139–147.
Pommerening, A., Svensson, A., Zhao, Z., Wang, H., Myllymäki, M., 2019. Spatial species diversity in temperate species-rich forest ecosystems: revisiting and extending the concept of spatial species mingling. Ecol. Indic. 105, 116–125.
Pommerening, A., Grabarnik, P., 2019. Individual-Based Methods of Forest Ecology and Management. Springer, Cham.
Pommerening, A., Wang, H., Zhao, Z., 2020a. Global woodland structure from local interactions: new nearest-neighbour functions for understanding the ontogenesis of global forest structure. For. Ecosyst. 7, 22.
Pommerening, A., Szmyt, J., Zhang, G., 2020b. A new nearest-neighbour index for monitoring spatial size diversity: the hyperbolic tangent index. Ecol. Model. 435, 109232.
Pommerening, A., Zhang, G., Zhang, X., 2021. Unravelling the mechanisms of spatial correlation between species and size diversity in forest ecosystems. Ecol. Indic. 121, 106995.
R Development Core Team, 2020. R: A Language and Environment for Statistical Computing. R Foundation for Statistical Computing, Vienna, Austria. http://www.r-project.org.
Torquato, S., 2002. Random Heterogeneous materials. Microstructure and macroscopic properties. Interdisciplinary Applied Mathematics. Springer, New York.
Wang, H., Peng, H., Hui, G., Hu, Y., Zhao, Z., 2018. Large trees are surrounded by more heterospecific neighboring trees in Korean pine broad-leaved natural forests. Sci. Rep. 8, 9149.
Wang, H., Zhao, Z., Myllymäki, M., Pommerening, A., 2020. Spatial size diversity in natural and planted forest ecosystems: revisiting and extending the concept of spatial size inequality. Ecol. Inform. 56, 101054.
Weiner, J., Solbrig, O.T., 1984. The meaning and measurement of size hierarchies in plant populations. Oecologia 61, 334–336.